Influence of pH and Protein Thermal Treatment on the Rheology of Pea Protein-Stabilized Oil-in-Water Emulsions

J.M. Franco*, P. Partal, D. Ruiz-M rquez, B. Conde, and C. Gallegos

Departamento de Ingeniería Química, Universidad de Huelva, Escuela Politécnica Superior, 21819, Huelva, Spain

ABSTRACT: The influence of emulsion pH and previous thermal treatment of the protein on the rheological behavior of pea protein-stabilized emulsions has been studied. Oil-in-water emulsions with 65% weight oil and 6% weight pea protein isolate were prepared. Emulsion pH was varied between 3.5 and 7.0. In addition to this, the protein aqueous phase was submitted to different previous thermal treatments by modifying temperature from 25 to 90°C and heating time from 20 to 60 min. To study the influence of the above-mentioned variables, droplet size distribution and steady-state flow curves were determined, and linear viscoelastic measurements were carried out. An increase in the pH of the emulsion initially leads to an increase in emulsion viscosity and viscoelastic functions, as well as to a decrease in the mean droplet size, up to an emulsion pH close to the protein isoelectric point, where a singular rheological behavior is found. An increase in temperature or heating time on the protein aqueous phase yields higher values of steady-state viscosity and linear viscoelasticity functions, up to a complete denaturation of the protein.

Paper no. J9495 in *JAOCS 77,* 975–983 (September 2000).

KEY WORDS: Emulsion, pea protein, pH, rheology, viscoelasticity, viscosity.

Vegetable proteins from a wide range of plant sources are extensively employed in human foods because of their nutritional and functional properties. They have been used in the form of protein isolates and concentrates as dairy and meat substitutes in a range of food products (1).

Oil-in-water emulsions are manufactured by dispersing the oil phase into the aqueous continuous phase in the form of small droplets, with most commercial emulsions having droplet sizes in the range of 0.1–10 μm (2). To obtain stable emulsions with suitable droplet size distributions (DSD), the emulsification process requires a considerable amount of mechanical energy, in the order of 1–100 MJ/m^3, depending on the emulsification machine (3). The emulsification process is a highly complex unit operation, which depends on many variables, such as residence time, agitation speed, and temperature (4).

An emulsifier is typically added to both improve the emulsification process and the emulsion stability. The emulsifier molecules adsorb at the oil–water interface and reduce the interfacial tension, thereby favoring emulsification and forming a protective barrier around the oil droplets (5). This induces a reduction of droplet size that increases interdroplet interactions and provides enhanced stability against coalescence. The role of these interactions is fundamental in highly concentrated emulsions, where droplets are tightly packed, and the continuous phase consists of a thin film separating adjacent droplets. This results in solid-like responses (6) and may lead to the development of an extensive flocculation of droplets to form a weak gel-like particulate network, depending on the nature and concentration of the emulsifier (7). The extensive flocculation process provides enhanced stability to the emulsion because the creaming rate is significantly decreased due to immobilization of the continuous phase (8,9). Consequently, stability, structural parameters, such as DSD and the nature and strength of interdroplet interactions, and the rheological behavior of emulsions are closely related, and all of them are influenced by the processing conditions (4).

Hence, protein adsorption at the fluid interfaces is of great importance for the food industry because it provides stability against phase separation in food systems, such as dairy products, baked food, ice creams, and mayonnaises. There is a close relationship between protein structure and protein functionality. However, the former is affected by many factors in the surrounding environment (i.e., pH, ionic strength, temperature, presence of other compounds), which makes it difficult to predict protein functionality and, therefore, the rheology in a given food system (10).

Therefore, environmental variables, such as pH or thermal treatments, may be considered important factors that affect the efficiency of the emulsification process and consequently the stability and physical properties of protein-stabilized emulsions. Taking this into account, the overall objective of this work was to study the effect that emulsion pH and previous thermal treatment, to which the protein aqueous phase was submitted, exert on the rheological behavior of pea protein-stabilized emulsions.

*To whom correspondence should be addressed at Departamento de Ingeniería Química, Universidad de Huelva, Escuela Politécnica Superior, Ctra. de Palos de la Frontera s/n, 21819, Huelva, Spain. E-mail: franco@uhu.es

TABLE 1
Technical Information on Pea Protein Isolate

Composition based on dry matter			
Proteins (N × 6.25)			90 ± 2%
Fats (extracted with petroleum ether)			Max. 0.5%
Ash			5 ± 1%
Sodium			0.7%
Calcium			0.15%
Phosphorus			0.52%
Magnesium			0.2%
Potassium			0.4%
Carbohydrates			Max. 4.5%
Dry matter (102°C)			95 ± 2%
Average amino acid content (g/100 g protein)			
Glycine	4.6	Phenylalanine	5.5
Alanine	4.7	Tryptophan	1.0
Valine	5.2	Proline	4.5
Leucine	8.0	Methionine	1.1
Isoleucine	4.6	Cysteine	1.2
Serine	5.4	Lysine	8.2
Threonine	4.1	Histidine	2.8
Tyrosine	4.1	Arginine	9.0
Aspartic acid	12.3	Glutamic acid	19.8

EXPERIMENTAL PROCEDURES

Different oil-in-water emulsions were prepared with a constant sunflower oil concentration (65% wt) and stabilized by a pea protein isolate, provided by Cosucra S.A. (Fontenoy, Belgium). Technical information on this isolate is given in Table 1. Protein concentration was fixed at 6% wt. Before the oil phase was added, protein isolate was dispersed in distilled water under different experimental conditions. Emulsion pH was varied between 3.5 and 7, by adding to the continuous phase different amounts of acetic acid. In addition to this, the protein solution was submitted to different previous thermal treatments by modifying temperature (between 25 and 90°C) and heating time (between 20 and 60 min). Oil-in-water emulsions were prepared in an Ultra-Turrax T-25 homogenizer from IKA (Staufen, Germany). Sunflower oil was added to the protein solution at room temperature and mixed at 8000 rpm for 5 min. Emulsions were stored at 5°C.

DSD measurements were performed in a Malvern Mastersizer-X (Malvern, United Kingdom). Dynamic viscoelasticity and steady-state flow tests were carried out in a controlled-stress rheometer (RS-100) from Haake (Karlsruhe, Germany). Oscillatory tests were performed inside the linear viscoelasticity region with a cone-and-plate sensor system (35 mm, 4°) in a frequency range of 10^{-2}–10^{2} rad/s. Linear viscoelastic ranges were analyzed by studying the stress dependence of the viscoelastic functions in stress sweep tests at 1 Hz. The critical stress values, above which the viscoelastic functions are dependent on the applied sinusoidal stress, are comprised between 2 and 15 Pa. Steady-state flow curves were obtained with a serrated plate-plate geometry (20 mm). As was previously found in the same type of emulsions (11), wall-slip effects can be avoided by using rough surfaces. At least three replicates of each test were made at 25°C. All samples had the same recent thermal and rheological history.

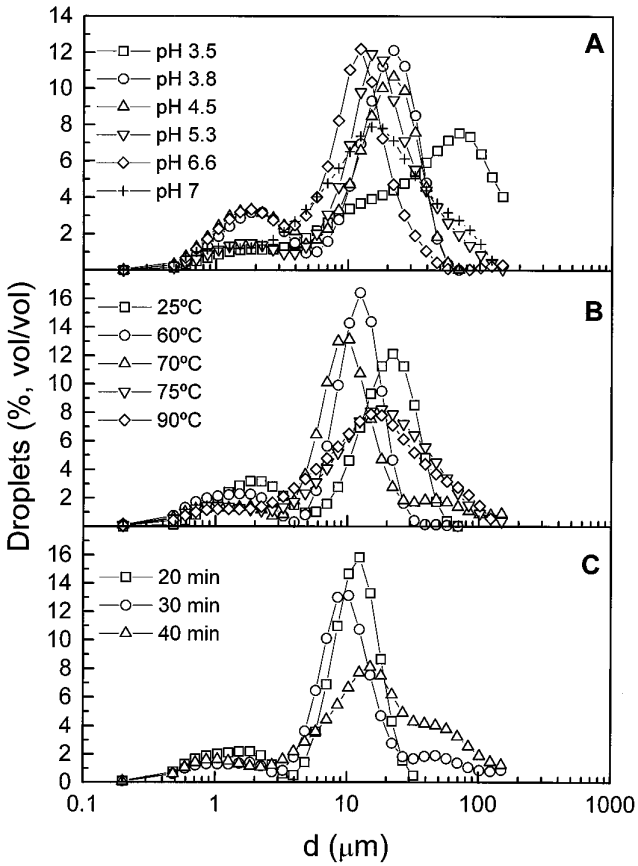

FIG. 1. Evolution of droplet size distribution (DSD) with (A) emulsion pH, (B) temperature applied to the protein aqueous phase, and (C) heating time for pea protein-stabilized emulsions.

RESULTS AND DISCUSSION

DSD. Figure 1 shows the effect of pH (Fig. 1A) and previous protein thermal treatment (Figs. 1B and 1C) on the DSD curves of these emulsions. All DSD curves show a bimodal shape, with a secondary maximum at relatively low values of the droplet diameter and the maximum distribution value at higher sizes, which generally moves to lower sizes as pH increases. The influence of protein thermal treatment is much more complicated.

The wide DSD found may be explained by taking into account the fact that, during the emulsification process, the disruption of oil droplets is followed by a coalescence process, which is favored by the intense mechanical energy supplied and a high temperature of emulsification (12). The low diffusion rate of macromolecules, such as proteins, favors a polydisperse DSD because the interfacial film necessary to prevent coalescence during emulsification is formed more slowly than the disruption of droplets.

Values of the Sauter diameter, d_{sv}, which is inversely proportional to the specific surface area of the droplets (13), have been obtained as follows:

$$d_{sv} = \frac{\sum n_i d_i^3}{\sum n_i d_i^2} \quad [1]$$

where n_i is the number of droplets with diameter d_i. Sauter's diameter is an appropriate structural parameter that dominates the flow behavior of concentrated emulsions (6), although it has also been related to linear viscoelasticity parameters (14,15). Table 2 shows values of the Sauter diameter for the different emulsions studied as a function of pH and thermal treatment.

Flow behavior. Steady-state flow curves of these emulsions (Fig. 2) always show a shear-thinning behavior, with a clear tendency to both a zero-shear rate-limiting viscosity, η_o, at low shear rates and, in some of them, a high-shear rate-limiting viscosity, η_∞. This behavior is closely related to a mechanism of oil droplet deflocculation in concentrated emulsions. This flow behavior has also been found in other types of emulsions, such as salad dressings (8,9) or highly concentrated emulsions (16,17). As was pointed out by several authors (9,11,17), the Carreau model fits the foregoing behavior fairly well:

$$\frac{\eta - \eta_\infty}{\eta_o - \eta_\infty} = \frac{1}{\left[1 + \left(\dot{\gamma}/\dot{\gamma}_c\right)^2\right]^n} \quad [2]$$

where $\dot{\gamma}_c$ is a critical shear rate for the onset of the shear-thinning region, and n is a parameter related to the slope of this intermediate region. The values of these fitting parameters are shown in Table 3 as a function of the different variables studied.

Dynamic viscoelastic measurements. Once the linear viscolastic region was established, frequency sweep tests were carried out at constant stress within the linear viscoelastic region. Evolution of the storage and loss moduli with frequency for all emulsions studied is shown in Figure 3. The storage modulus, G′, is always higher than the loss modulus, G″, within the experimental frequency range. Hence, the emulsions present a predominantly elastic response, showing an apparent plateau region in the experimental frequency range studied. The appearance of this plateau region has been related to an extensive flocculation process due to interactions among the emulsifier molecules located at the oil–water interface of adjacent droplets (7,9). This behavior is typically found in highly concentrated emulsions, such as commercial

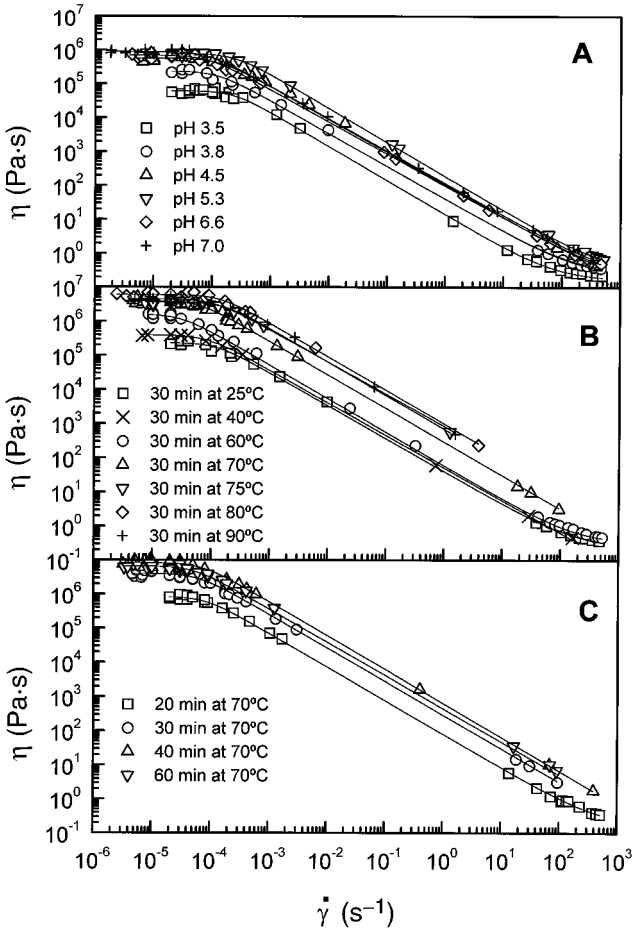

FIG. 2. Evolution of the steady-state flow curves with (A) emulsion pH, (B) temperature applied to the protein aqueous phase, and (C) heating time for pea protein-stabilized emulsions. η, viscosity, $\dot{\gamma}$= shear rate.

TABLE 2
Values of Sauter s Mean Diameter (d_{sv}) for the Emulsions Studied

pH	Heating temperature (ºC)	Heating time (min)	d_{sv}[a] (μm)
3.5	25	—	10.11
3.8	25	—	5.75
4.5	25	—	4.82
5.3	25	—	7.89
6.6	25	—	4.54
7	25	—	4.74
3.8	60	30	4.51
3.8	70	30	5.48
3.8	75	30	6.22
3.8	90	30	6.39
3.8	70	20	4.58
3.8	70	40	5.82

[a]See Equation 1.

TABLE 3
Carreau Model Parameters for the Emulsions Studied

pH	Heating temperature (ºC)	Heating time (min)	η_o (Pa·s)	$\dot{\gamma}_c$ (s^{-1})	n	η_∞ (Pa·s)
3.5	25	—	$6.11 \cdot 10^4$	$2.3 \cdot 10^{-4}$	0.5	0.17
3.8	25	—	$2.34 \cdot 10^5$	$1.2 \cdot 10^{-4}$	0.48	0.24
4.5	25	—	$5.67 \cdot 10^5$	$1.3 \cdot 10^{-4}$	0.48	0.14
5.3	25	—	$7.72 \cdot 10^5$	$2.4 \cdot 10^{-4}$	0.5	0.29
6.6	25	—	$6.95 \cdot 10^5$	$8 \cdot 10^{-5}$	0.47	0.2
7	25	—	$9.02 \cdot 10^5$	$8 \cdot 10^{-5}$	0.475	0.25
3.8	40	30	$4.01 \cdot 10^5$	$8 \cdot 10^{-5}$	0.48	0.21
3.8	60	30	$1.6 \cdot 10^6$	$3 \cdot 10^{-5}$	0.49	0.32
3.8	70	30	$4.03 \cdot 10^6$	$6 \cdot 10^{-5}$	0.49	—
3.8	75	30	$3.68 \cdot 10^6$	$1.6 \cdot 10^{-4}$	0.49	—
3.8	80	30	$6 \cdot 10^6$	$1.4 \cdot 10^{-4}$	0.49	—
3.8	90	30	$4.4 \cdot 10^6$	$1.3 \cdot 10^{-4}$	0.47	—
3.8	70	20	$8.38 \cdot 10^5$	$8 \cdot 10^{-5}$	0.49	0.17
3.8	70	40	$8.4 \cdot 10^6$	$7 \cdot 10^{-5}$	0.49	—
3.8	70	60	$6.74 \cdot 10^6$	$5 \cdot 10^{-5}$	0.48	—

[a]See Equation 2.

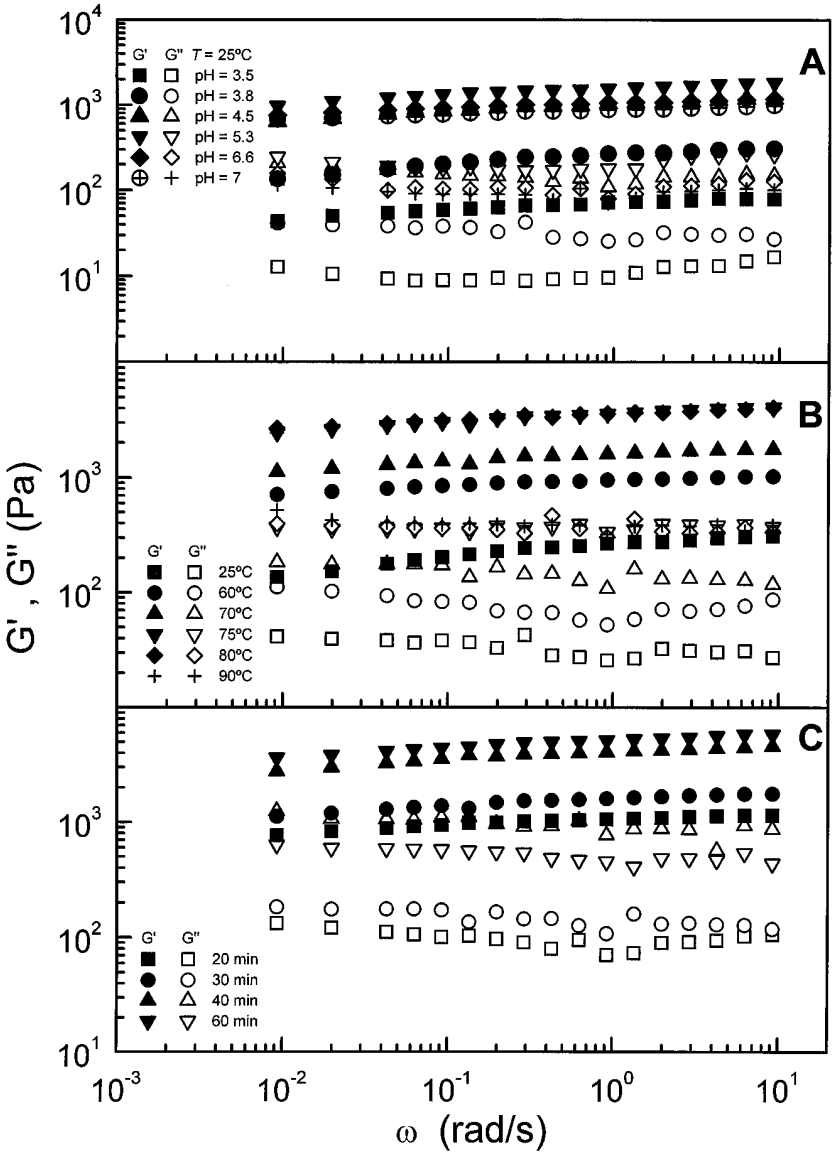

FIG. 3. Influence of (A) emulsion pH, (B) temperature applied to the protein aqueous phase, and (C) heating time on the linear viscoelasticity functions for pea protein-stabilized emulsions. G′ = storage modules, G″ = loss modulus, ω = frequency.

or model mayonnaises (18,19) and salad dressing-type emulsions (20,21). When the emulsion is only stabilized by proteins (17–19), a more pronounced plateau region is observed, which is related to the formation of a three-dimensional network due to entanglements among protein segments adsorbed at the oil–water interface.

In the plateau region, the loss tangent passes through a minimum, which has been used to calculate an approximate value of the plateau modulus, G_N° (21–23). The plateau modulus is a viscoelastic parameter, defined as an extrapolation of the entanglement contribution to G′ at high frequencies (24). This parameter may be estimated from the minimum in tan δ as follows (22):

$$G_N^\circ = [G']_{\tan\delta \rightarrow \text{minimum}} \quad [3]$$

The influence that pH and thermal treatment exert on the linear viscoelastic behavior of these emulsions will be discussed taking into account the evolution of the plateau modulus with the above-mentioned variables.

Influence of pH. As shown in Figure 2A, the flow curves of these emulsions are always quite similar in shape, a trend to reach a zero-shear rate-limiting viscosity and no significant differences in the slope of the shear-thinning region (Table 3). As has been previously reported (8,25), this fact makes possible the application of a superposition method to obtain a master flow curve, using a dimensionless viscosity and a shifted shear rate by using an empirically calculated shift factor. Val-

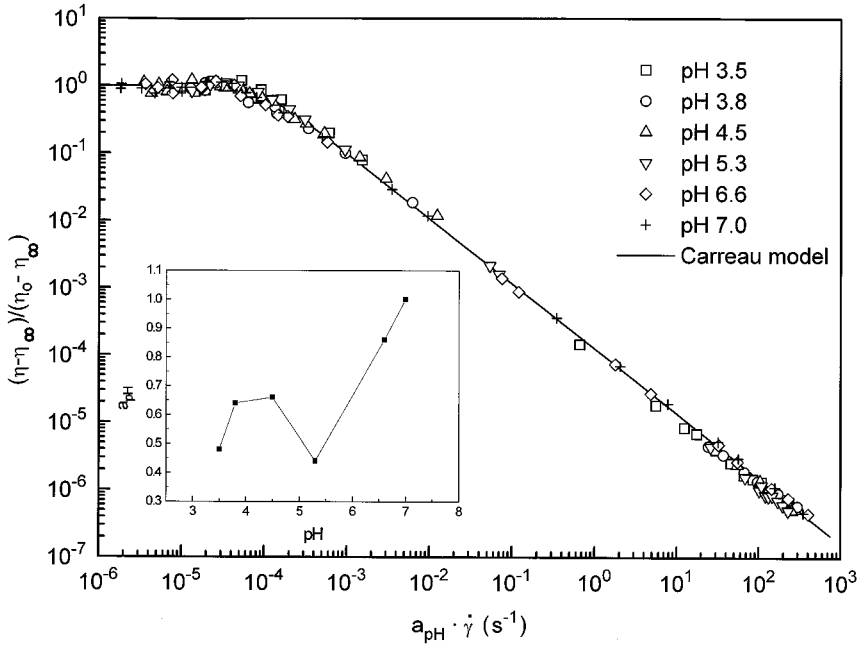

FIG. 4. pH-Reduced master flow curve and evolution of the shift factor with emulsion pH for pea protein-stabilized emulsions. See Equation 4.

ues of the shift factors for the different emulsions studied, as a function of pH, are shown in Figure 4. A dimensionless viscosity, including both the zero-shear rate and the high-shear rate-limiting viscosities, obtained from the fitting of the Carreau model, was used. Thus, $\eta_{red} = (\eta - \eta_\infty)/(\eta_o - \eta_\infty)$ vs. $a_{pH}\cdot\dot{\gamma}$ leads to an empirical master curve that describes the flow behavior of these emulsions in the range of pH studied, where a_{pH} is the empirical shift factor (Fig. 4), which is equal to 1 for the reference flow curve (pH = 7). The master flow curve obtained may be described by a modified Carreau model, as follows:

$$\eta_{red} = \frac{1}{\left[1+\left(a_{pH}\cdot\dot{\gamma}/\dot{\gamma}_{c,pH_o}\right)^2\right]^{n_{pH_o}}} \quad [4]$$

where $\dot{\gamma}_{c,pH_o}$ and n_{pH_o} are the values of Carreau model parameters at the pH of reference.

Moreover, pH dependence of the shift factor must provide information about the influence of emulsion pH on viscous behavior. As may be deduced from Equation 4, a_{pH} is related to the critical shear rate for the onset of the shear-thinning region, $\dot{\gamma}_c$. Consequently, this parameter gives information

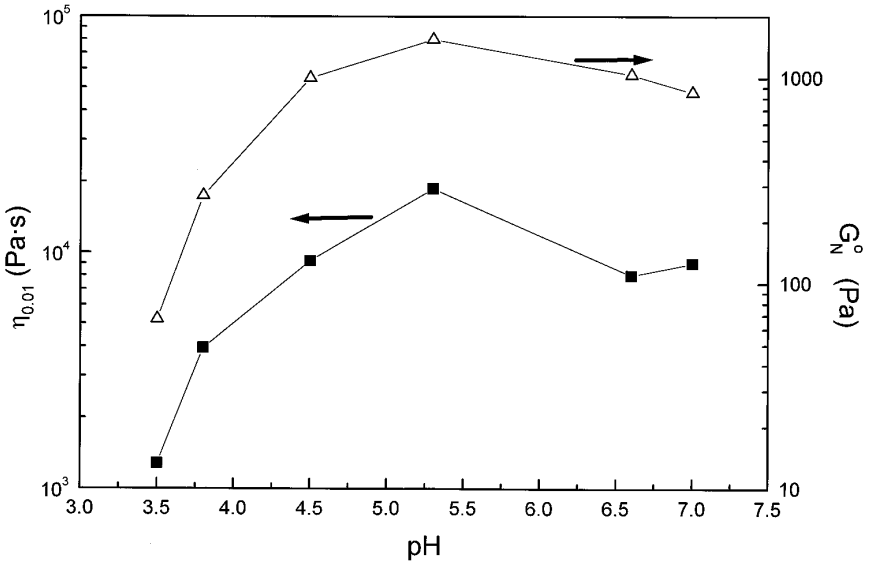

FIG. 5. Evolution of the steady-state viscosity at 0.01 s^{-1} and the plateau modulus (G_N°) with emulsion pH for pea protein-stabilized emulsions.

about the resistance of the emulsion microstructure to a shear-induced breakdown process.

Figure 5 shows the evolution of the steady-state viscosity, at 0.01 s^{-1}, with emulsion pH. This viscosity, well inside the experimental shear-rate range studied, is much more reliable than the zero-shear rate-limiting viscosity, which is obtained at low shear rates and with a high level of uncertainty. Steady-state flow viscosity undergoes an initial increase with pH up to a maximal value at an emulsion pH value of 5.3, close to the isoelectric point of the protein. A slight decrease in viscosity is then observed at higher pH values. A similar tendency may be found by studying the linear viscoelasticity functions of these emulsions. Thus, if the plateau modulus values are analyzed (see Fig. 5), a maximum in this parameter is also found for a pH value of 5.3. In relationship to the evolution of droplet size with emulsion pH, there is an initial continuous decrease in the Sauter diameter as pH increases, a fact that would explain the increase in the viscous and viscoelastic functions. The larger values of Sauter's diameter as emulsion pH decreases are closely related to the lower diffusion rate of the protein to the oil–water interface, due to a higher denaturation degree of the protein as pH decreases (26). Nevertheless, a dramatic change in this tendency is observed at a pH of 5.3, which shows a significantly higher value of the Sauter diameter (Table 2). A further increase in pH leads to lower droplet sizes and narrower distributions. Both factors should lead to an increase in emulsion viscosity (27). However, it has been previously demonstrated (17,21,28) that DSD is not the only structural parameter to affect the rheology of emulsions, especially in highly structured macromolecule-stabilized systems, in which interdroplet interactions may play a key role. The results previously shown may be explained by taking into account that at the isoelectric point, the pea protein isolate has its lowest solubility (1,29). Thus, when pea protein/water systems at different pH are centrifuged, three different phases were always obtained: an undissolved protein fraction (upper phase), an intermediate aqueous solution, and a gel-like viscous phase (bottom phase). The binary system with a pH close to the protein isoelectric point shows the maximal undissolved protein fraction (upper phase) and the least gel-like phase (bottom phase). Obviously, the poor solubility of the protein around this pH significantly reduces the effective concentration of pea protein able to be adsorbed at the interface and, consequently, according to our results, the Sauter diameter must increase. However, Waniska and Kinsella (26) showed that rates of adsorption and packing of β-lactoglobulin in the interfacial film were maximum near the isoelectric point, reflecting the minimum electrostatic repulsion between proteins at the interface. A highly packed protein film at the interface leads to a high surface viscoelasticity, which is closely related to the bulk rheology of the emulsion (30,31) and the emulsifying capacity (32). This explains why at an emulsion pH of 5.3, near the isoelectric point of the protein, higher values of emulsion viscosity and viscoelastic parameters than those expected from its DSD may be found. Moreover, the shift factor that affects shear rates in the master curve obtained passes through an important minimum value at pH 5.3 (Fig. 4). This indicates that the emulsion microstructure at a pH close to the isoelectric point of the protein shows a significantly higher shear resistance than that found for other emulsion pH values. This value of the shift factor is only comparable to that found for the emulsion with a pH of 3.5, which shows the largest Sauter diameter and the lowest values of steady-state viscosity and plateau modulus, although the protein is largely denatured. The further slight decrease in the viscous and viscoelastic functions, at emulsion pH values above 5.3, should be related to a decrease in interfacial viscoelasticity, in spite of lower Sauter's diameter.

Influence of protein thermal treatment. A more severe thermal treatment of the protein aqueous phase, i.e., higher temperature or longer heating time, leads to more viscous emulsions (Figs. 2B and 2C). As shown in these figures (emulsion pH = 3.8), the flow curves show a similar shape and no significant differences in the slope of the shear-thinning region (see Table 3). As a result, a plot of a dimensionless viscosity, $\eta_{red} = (\eta - \eta_\infty)/(\eta_o - \eta_\infty)$ vs. $a_{H(T)} \cdot a_{H(t)} \cdot \dot{\gamma}$ leads again to an empirical master curve that describes the flow behavior of the emulsion under these previous thermal treatment conditions (Fig. 6). The shift factors, $a_{H(T)}$ and $a_{H(t)}$, are related, respectively, to the previous temperature and heating time applied to the protein aqueous phase, and both of them are equal to 1 for the reference flow curve (pH = 3.8, 30 min and 70°C). A modified Carreau model, expressed as follows, may describe the master flow curve:

$$\eta_{red} = \frac{1}{\left[1 + \left(a_{H(T)} \cdot a_{H(t)} \cdot \dot{\gamma} / \dot{\gamma}_{c,H_o}\right)^2\right]^{n_{H_o}}} \quad [5]$$

where $\dot{\gamma}_{c,H_o}$ and n_{H_o} are the values of Carreau model parameters at the reference treatment conditions.

The evolution of $a_{H(T)}$ with temperature is shown in Figure 6, where a maximum value corresponding to a temperature around 60°C is observed. On the contrary, $a_{H(t)}$ is constant in the range of heating time studied. As a result, while the previous temperature applied on the protein aqueous phase has a remarkable effect on the resistance of the emulsion structural network, heating time seems not to modify this resistance, although the emulsion viscosity significantly increases.

Figures 7 and 8 show the evolution of the steady-state viscosity at 0.01 s^{-1}, and the plateau modulus with temperature and heating time, respectively. As shown in Figure 7, both rheological parameters dramatically increase up to a temperature around 75°C, a fact that has been reported to be closely related to an extensive denaturation of the protein (28). High temperatures applied during the emulsification process may exert the same effects (9,33). As Arntfield and Murray (34) have demonstrated, by using differential scanning calorimetric (DSC) measurements, pea protein denatures at a lower temperature (around 85°C) than other vegetable proteins. At low pH values, the temperature-induced conformational

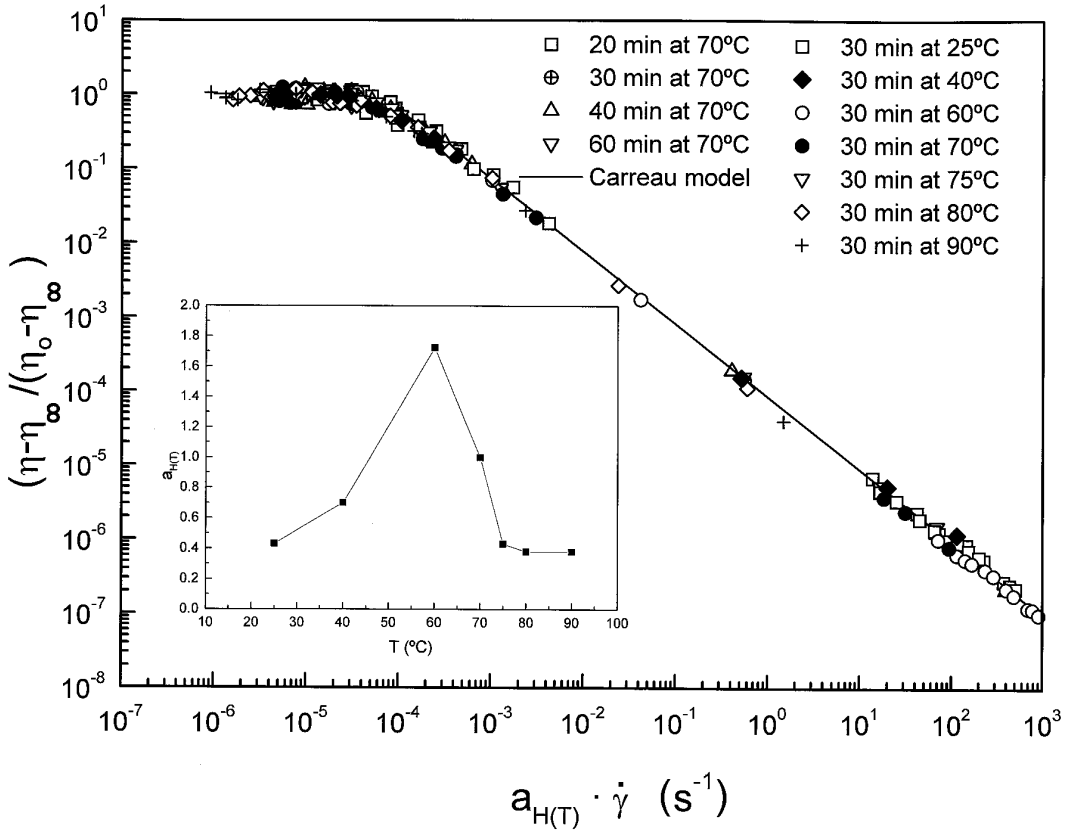

FIG. 6. Temperature and heating time-reduced master flow curve and evolution of the shift factor with temperature for pea protein-stabilized emulsions. See Equation 5.

changes of the protein are dampened, reflected in a lower enthalpy of denaturation (1,34). A decrease in protein pH decreases the denaturation temperature down to around 70°C at pH 3.8, which is in concordance with the rheological results obtained (increase in $\eta_{0.01}$ and G_N° and decrease in $a_{H(T)}$) and the increase in Sauter's diameter when temperature rises from 60 to 70°C. The above-mentioned denaturation may also be clearly observed after centrifugation, where an extended gel-

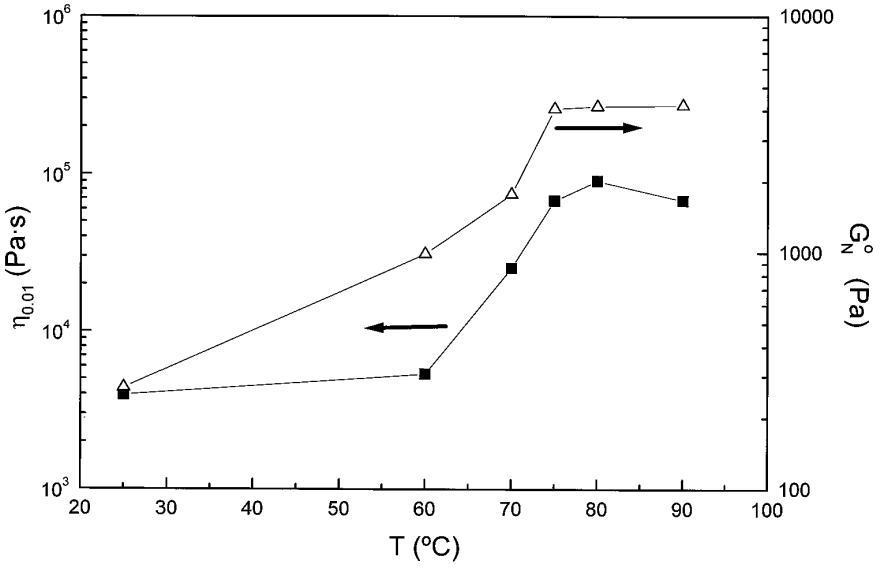

FIG. 7. Evolution of steady-state viscosity at 0.01 s^{-1} and plateau modulus with temperature applied to the protein aqueous phase for pea protein-stabilized emulsions.

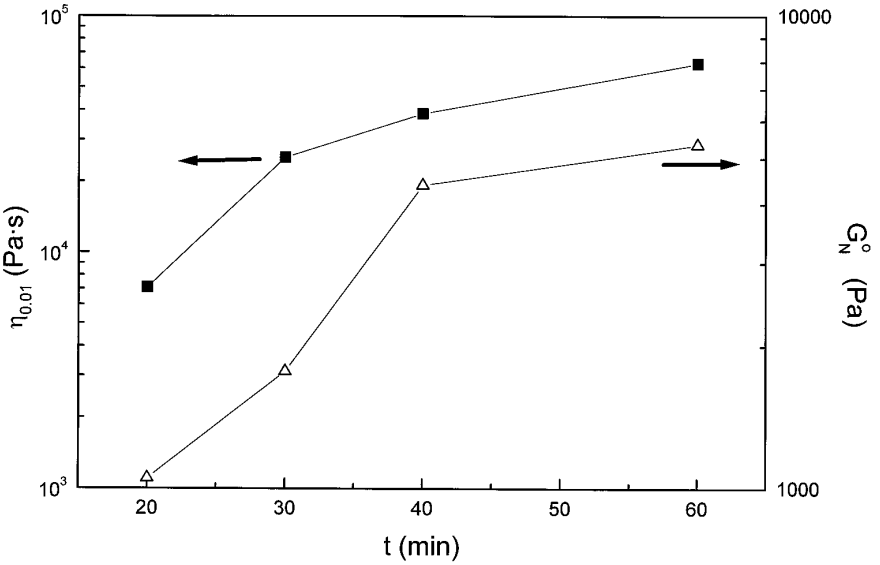

FIG. 8. Evolution of steady-state viscosity at 0.01 s^{-1} and plateau modulus with heating time for pea protein-stabilized emulsions.

like phase is found for this protein aqueous phase (pH = 7.0, 80°C). In addition to this, as Raymundo *et al.* (28) have reported, an increase in heating time applied to the protein aqueous phase, at a constant temperature, may exert an important effect on the rheological properties of vegetable protein-stabilized emulsions. As shown in Figure 8, the emulsion steady-state viscosity at 0.01 s^{-1} and the plateau modulus initially increase with protein heating time, showing a tendency to reach constant values of these rheological parameters at sufficiently long protein heating times, when protein denaturation has been completed.

REFERENCES

1. Bacon, J.R., T.R. Noel, and N. Lambert, Preparation of Transparent Pea Proteins Gel: A Comparison of Isolation Procedures, *Int. J. Food Sci. Technol. 25*:527–537 (1990).
2. Walstra, P., Formation of Emulsions, in *Encyclopedia of Emulsion Technology,* Vol. 1, edited by P. Becher, Marcel Dekker, New York, 1983, pp. 57–127.
3. Walstra P., Principles of Emulsion Formation, *Chem. Eng. Sci. 48*:333–349 (1993).
4. Gallegos, C., and J.M. Franco, Rheology of Food Emulsions, in *Advances in the Flow and Rheology of Non-Newtonian Fluids*, edited by D. Siginer, D. De Kee, and R.P. Chhabra, Elsevier, Amsterdam, 1999, pp. 87–118.
5. Dickinson, E., Interactions in Protein-Stabilized Emulsions, in *Progress and Trends in Rheology IV*, edited by C. Gallegos, Steinkopff, Darmstadt, Germany, 1994, pp. 227–230.
6. Otsubo, Y., and R.K. Prud'homme, Rheology of Oil-in-Water Emulsions, *Rheol. Acta 33*:29–37 (1994).
7. Dickinson, E., Food Colloids—An Overview, *Colloids Surf. 42*:191–204 (1989).
8. Franco, J.M., and M. Berjano, A. Guerrero, J. Muñoz, and C. Gallegos, Flow Behaviour and Stability of Light Mayonnaise Containing a Mixture of Egg Yolk and Sucrose Stearate as Emulsifiers, *Food Hydrocoll. 9*:111–121 (1995).
9. Franco, J.M., A. Guerrero, and C. Gallegos, Rheology and Processing of Salad Dressing Emulsions, *Rheol. Acta 34*:13–524 (1995).
10. Toro-Vazquez, J.F., and J.M. Regenstein, Physicochemical Parameters of Protein Additives and Their Emulsifying Properties, *J. Food Sci. 54*:1177–1201 (1989).
11. Franco, J.M., C. Gallegos, and H.A. Barnes, On Slip Effects in Steady-State Flow Measurements of Oil-in-Water Food Emulsions, *J. Food Eng. 36*:89–102 (1998).
12. Gallegos, C., M.C. Sanchez, A. Guerrero, and J.M. Franco, Microstructure, Rheology and Processing of Emulsions, in *Rheology and Fluid Mechanic of Nonlinear Materials,* edited by D.A. Siginer, AMD, Vol. 217, 1996, pp. 177–183.
13. Sprow, F.B., Distribution of Drop Sizes Produced in Turbulent Liquid-Liquid Dispersion, *Chem. Eng. Sci. 22*:435–442 (1967).
14. Princen, H.M., and A.D. Kiss, Rheology of Foams and Highly Concentrated Emulsions, *J. Colloid Interface Sci. 112*:427–444 (1986).
15. Partal, P., A. Guerrero, and C. Gallegos, Linear Viscoelastic Properties of Sucrose Ester-Stabilized Oil-in-Water Emulsions, *J. Rheol. 42*:1375–1388 (1998).
16. Otsubo, Y., and R.K. Prud'homme, Effect of Drop Size Distribution on the Flow Behavior of Oil-in-Water Emulsions, *Rheol. Acta 33*:303–306 (1994).
17. Franco, J.M., A. Raymundo, I. Sousa, and C. Gallegos, Influence of Processing Variables on the Rheological and Textural Properties of Lupin Protein-Stabilized Emulsions, *J. Agric. Food Chem. 46*:3109–3115 (1998).
18. Gallegos, C., M. Berjano, and L. Choplin, Linear Viscoelastic Behaviour of Commercial and Model Mayonnaise, *J. Rheol. 36*:465–478 (1992).
19. Guerrero, A., and H.R. Ball, Effect of the Spray-Dried or Reduced-Cholesterol Yolk and Temperature on the Linear Viscoelastic Properties of Mayonnaise, *J. Texture Stud. 25*:363–381 (1994).
20. Muñoz, J., and P. Sherman, Dynamic Viscoelastic Properties of Some Commercial Salad Dressings, *Ibid. 21*:411–426 (1992).
21. Franco, J.M., M. Berjano, and C. Gallegos, Linear Viscoelasticity of Salad Dressing Emulsions, *J. Agric. Food Chem. 45*: 713–719 (1997).

22. Wu, S., Chain Structure and Entanglement, *J. Polym. Sci. 27*: 723–741 (1989).
23. Arendt, B.H., R.M. Kannan, M. Zewail, J.A. Kornfield, and S.D. Smith, Dynamic of Each Component in Miscible Blends of Polyisoprene and Polyvinylethylene, *Rheol. Acta 33*:322–336 (1994).
24. Baumgaertel, M., M.E. De Rosa, J. Machado, M. Masse, and H.H. Winter, The Relaxation Time Spectrum of Nearly Monodisperse Polybutadiene Melts, *Ibid. 31*:75–82 (1992).
25. Partal, P., A. Guerrero, M. Berjano, and C. Gallegos, Influence of Concentration and Temperature on the Flow Behavior of Oil-in-Water Emulsions Stabilized by Sucrose Palmitate, *J. Am. Oil. Chem. Soc. 74*:1203–1212 (1997).
26. Waniska, R.D., and J.E. Kinsella, Surface Properties of β-Lactoglobulin: Adsorption and Rearrangement During Film Formation, *J. Agric. Food Chem. 33*:1143–1148 (1985).
27. Rahalkar, R.R., Viscoelastic Properties of Oil-Water Emulsions, in *Viscoelastic Properties of Foods,* edited by M.A. Rao and J.F. Steffe, Elsevier Applied Science, London, 1992, pp. 317–354.
28. Raymundo, A., J.M. Franco, C. Gallegos, J. Empis, and I. Sousa, Effect of Thermal Denaturation of Lupin Protein on Its Emulsifying Properties, *Nahrung 42*:220–224 (1998).
29. Sosulski, F.W., and A.R. McCurdy, Functionally of Flours, Protein Fractions and Isolates from Field Peas and Faba Bean, *J. Food Sci. 52*:1010–1014 (1987).
30. Rivas, H.J., and P. Sherman, Soy and Meat Proteins as Food Emulsion Stabilizers. 1. Viscoelastic Properties of Corn Oil-in-Water Emulsions Incorporating Acid Precipitated Soy or Meat Proteins, *J. Texture Stud. 14*:251–265 (1983).
31. Dickinson, E., and S.T. Hong, Influence of Water-Soluble Nonionic Emulsifier on the Rheology of Heat-Set Protein Stabilized Emulsion Gels, *J. Agric. Food Chem. 43*:2560–2566 (1995).
32. Elizalde, B.E., G.B. Bartholomai, and A.M.R. Pilosof, The Effect of pH on the Relationship Between Hydrophilic/Lipophilic Characteristics and Emulsification Properties of Soy Proteins, *Lebens. Wiss. Technol. 29*:334–339 (1996).
33. Rivas, H.J., and P. Sherman, Soy and Meat Proteins as Food Emulsion Stabilizers. 2. Influence of Emulsification Tempera-

ture, NaCl and Methanol on the Viscoelastic Properties of Corn Oil-in-Water Emulsions Incorporating Acid Precipitated Soy Protein, *J. Texture Stud. 14*:267–275 (1983).
34. Arntfield, S.D., and D. Murray, The Influence of Processing Parameters on Food Protein Functionality. I. Differential Scanning Calorimetry as an Indicator of Protein Denaturation, *Can. Inst. Food Technol. J. 14*:289–294 (1981).

[Received January 3, 2000; accepted June 21, 2000]